Original Article

MOLECULAR METABOLISM

The human batokine EPDR1 regulates β-cell metabolism and function

Luis Rodrigo Cataldo [1,2,3,*], Qian Gao [1], Lidia Argemi-Muntadas [1], Ondrej Hodek [4], Elaine Cowan [2,3], Sergey Hladkou [2,3], Sevda Gheibi [2,3], Peter Spégel [2], Rashmi B. Prasad [2,3], Lena Eliasson [2,3], Camilla Scheele [1], Malin Fex [2,3], Hindrik Mulder [2,3], Thomas Moritz [1,4,*]

ABSTRACT

Objective: Ependymin-Related Protein 1 (EPDR1) was recently identified as a secreted human batokine regulating mitochondrial respiration linked to thermogenesis in brown fat. Despite that EPDR1 is expressed in human pancreatic β-cells and that glucose-stimulated mitochondrial metabolism is critical for stimulus-secretion coupling in β-cells, the role of EPDR1 in β-cell metabolism and function has not been investigated.
Methods: *EPDR1* mRNA levels in human pancreatic islets from non-diabetic (ND) and type 2 diabetes (T2D) subjects were assessed. Human islets, EndoC-βH1 and INS1 832/13 cells were transfected with scramble (control) and *EPDR1* siRNAs (*EPDR1*-KD) or treated with human EPDR1 protein, and glucose-stimulated insulin secretion (GSIS) assessed by ELISA. Mitochondrial metabolism was investigated by extracellular flux analyzer, confocal microscopy and mass spectrometry-based metabolomics analysis.
Results: *EPDR1* mRNA expression was upregulated in human islets from T2D and obese donors and positively correlated to BMI of donors. In T2D donors, *EPDR1* mRNA levels negatively correlated with HbA1c and positively correlated with GSIS. *EPDR1* silencing in human islets and β-cell lines reduced GSIS whereas treatment with human EPDR1 protein increased GSIS. *Epdr1* silencing in INS1 832/13 cells reduced glucose- and pyruvate- but not K^+-stimulated insulin secretion. Metabolomics analysis in *Epdr1*-KD INS1 832/13 cells suggests diversion of glucose-derived pyruvate to lactate production and decreased malate-aspartate shuttle and the tricarboxylic acid (TCA) cycle activity. The glucose-stimulated rise in mitochondrial respiration and ATP/ADP-ratio was impaired in *Epdr1*-deficient cells.
Conclusion: These results suggests that to maintain glucose homeostasis in obese people, upregulation of EPDR1 may improve β-cell function via channelling glycolysis-derived pyruvate to the mitochondrial TCA cycle.

Keywords Mitochondrial metabolism; Lactate; TCA cycle; Beta cells; Insulin secretion; Type 2 diabetes

1. INTRODUCTION

Type 2 Diabetes (T2D) results from an incapacity of β-cells to secrete sufficient amounts of insulin to compensate for peripheral insulin resistance. Glucose-induced mitochondrial metabolism is central for the stimulus-secretion coupling mechanism [1]. Thus, alteration of mitochondrial metabolism in pancreatic β-cells impairs the glucose-stimulated insulin secretion (GSIS) [2] and is a hallmark of T2D [3]. Therefore, a comprehensive understanding of glucose-induced β-cell mitochondrial metabolism is required to fully clarify the pathophysiology of T2D.

EPDR1 was first reported as the "mammalian homolog of ependymins" (MERP1) in 2001 [4]. Ependymins are glycoproteins synthetized by fibroblasts and secreted into cerebrospinal fluids in fish [4]. Genetically, *EPDR1* has been implicated in disease, including several types of cancer [5–8], osteoporosis [9], Dupuytren's disease [10,11] and primary angle closure glaucoma [12,13]. Despite this notion, the role of EPDR1 in human physiology remain elusive.
The crystal structure of human EPDR1 revealed hydrophobic binding grooves that can interact with lipids, suggesting a potential role of EPDR1 in lipid transport or degradation [14]. Proteomics studies of mammalian mannose-6-phosphate (M6P) glycoproteins have

[1]The Novo Nordisk Foundation Centre for Basic Metabolic Research, Faculty of Health and Medical Sciences, University of Copenhagen, Copenhagen, DK-2200 Denmark [2]Lund University Diabetes Centre, Clinical Research Center, Sweden [3]Department of Clinical Sciences in Malmö, Lund University, Sweden [4]Department of Forest genetics and Plant Physiology, Swedish University of Agricultural Sciences, Umeå, Sweden

*Corresponding authors. Novo Nordisk Foundation Center for Basic Metabolic Research University of Copenhagen Blegdamsvej 3B 2200 Copenhagen Maersk Tower, Room 7-8, Denmark.

E-mails: rodrigo.cataldo@med.lu.se (L.R. Cataldo), qian.gao@sund.ku.dk (Q. Gao), lidia.argemi.muntadas@sund.ku.dk (L. Argemi-Muntadas), ondrej.hodek@slu.se (O. Hodek), elaine.cowan@med.lu.se (E. Cowan), sergey.hladkou@med.lu.se (S. Hladkou), sevda.gheibi@med.lu.se (S. Gheibi), peter.spegel@chem.lu.se (P. Spégel), rashmi.prasad@med.lu.se (R.B. Prasad), lena.eliasson@med.lu.se (L. Eliasson), cs@sund.ku.dk (C. Scheele), malin.fex@med.lu.se (M. Fex), hindrik.mulder@med.lu.se (H. Mulder), thomas.moritz@sund.ku.dk (T. Moritz).

Received July 2, 2022 • Revision received October 14, 2022 • Accepted November 1, 2022 • Available online 5 November 2022

https://doi.org/10.1016/j.molmet.2022.101629

identified EPDR1 as a lysosomal protein with unknown function [15–17]. The lysosomal localization of EPDR1 was further demonstrated in mouse brain homogenates by subcellular fractionation [18]. Recently, another proteomics-based study, identified EPDR1 as a protein secreted by hBAT, suggesting that EPDR1 is a novel human batokine [19]. The protein was detected in human plasma samples suggesting it is involved in metabolic crosstalk between tissues [17]. *EPDR1*-silencing in human brown adipocytes reduces norepinephrine (NE)-induced mitochondrial proton-leak respiration and affects the expression of mitochondrial proteins [19]. Collectively, these data suggest that EPDR1 regulates whole-body energy metabolism by modulating mitochondrial metabolism in target cells.

RNAseq analysis of purified human fetal and adult pancreatic islet cells, shows low *EPDR1* mRNA levels in fetal α and β-cells. In contrast, in adult β-cells, its expression increases whereas it decreases in adult α-cells [20]. These data suggest that EPDR1 may play a role in mature β-cell function and may contribute to maintenance of glucose homeostasis *in vivo*.

In the present study, we have studied the role of EPDR1 in regulating β-cell metabolism and function in human pancreatic islets and β-cell models. Our data indicate that EPDR1 is required for adequate GSIS, participating in a mechanism to channel glucose metabolism via the mitochondrial TCA cycle. We propose that EPDR1 is critical in maintaining β-cell glucose-responsiveness under increased metabolic demands imposed by obesity.

2. RESEARCH DESIGN AND METHODS

2.1. Human pancreatic Islet cohort

Human pancreatic islets (n = 188) were obtained from the EXODIAB Human Tissue Laboratory, which receives islets from the Nordic Network for Clinical Islet Transplantation (http://www.nordicislets.org). The Clinical characteristics of the donors of islets and all methodological details related to RNA sequencing and genome-wide genotyping in islets from this cohort (188 donors) have recently been published [21]. For the correlational analysis of *EPDR1* mRNA levels with different metabolic/functional parameters separated by disease status and with the purpose of ensure high quality data, a subgroup of donors was filtered under the following criteria: islets with purity$\geq$70% and with days in culture$\leq$5. The characteristics of donors for this specific subgroup is shown in Table S1.

2.2. Cell culture

INS1 832/13 and EndoC-βH1 cells were cultured as previously described [22,23]. EndoC-βH1 cells were cultured in Matrigel/fibronectin-coated (100/2 mg/mL, Sigma-Aldrich) flasks with DMEM containing 5.6 mmol/L glucose, 2% BSA, 10 mmol/L nicotinamide, 50 mmol/L β-mercaptoethanol, 5.5 mg/mL transferrin, 6.7 ng/mL sodium selenite, 100 IU/mL penicillin, and 100 mg/mL streptomycin at 37 °C in a humidified atmosphere with 5% CO_2.

2.3. GSIS in β-cell lines and human islets

INS1 832/13 cells (1.7×10^5 cells/cm^2) and EndoC-βH1 cells (1.5×10^5 cells/cm^2) were seeded in 24 and 48 well-plates, respectively, 96 h before experiments were performed. Seeded cells and human pancreatic islets (10 islets/well, 24-WP, 4–6 replicates/condition) were starved in secretion assay buffer (SAB) buffer (final SAB 1X composition was (in mM): 114 NaCl; 4.7 KCl; 1.2 KH2PO4; 1.16 MgSO4; 20 HEPES; 2.5 CaCl2; 25.5 NaHCO3; 0.2% bovine serum albumin (BSA), pH 7.2–7.4) with low glucose (LG, 1–2.8 mM). Then, cells and islets were simultaneously (in parallel wells) stimulated for 1 h with SAB with LG, high glucose (HG, 16.7–20 mM) or HG+3-isobutyl-1-methylxanthine (IBMX) (100 μM). The insulin concentration in the supernatants (accumulated for 1 h of stimulation) was measured using the insulin ELISA: for samples from INS1 832/13 cells (non-diluted) High Range Rat Insulin ELISA (Mercodia, catalogue number (#): 10-1145-01), for samples from EndoC-βH1 cells (dilution factor: 12.5) and from human islets (dilution factor: 5) the Human Insulin Elisa (Mercodia, #10-1113-10). In EndoC-βH1 cells and human islets, the total insulin content was measured by extracting total cells/islet protein with RIPA buffer (composition was: 150 mM NaCl, 1% NP40, 0.5% sodium deoxycholate, 0.1% SDS, 50 mM TRIS–HCl, pH 8.0) and insulin secretion was normalized to the total insulin content and expressed as % secreted insulin.

2.4. EPDR1 protein treatment and silencing of β-cell lines and human islets

INS1 832/13 cells (1.7×10^5 cells/cm^2) and EndoC-βH1 cells (1.5×10^5 cells/cm^2) were seeded in 24 and 48 well-plates whereas 400–500 human pancreatic islets by condition were seeded in 35 mm petri dish and treated with vehicle (PBS) or with increasing concentrations (1.25–10 μg/mL) of human recombinant EPDR1 protein (UNIPROT entry Q9UM22, isoform 1, amino acids 39–224 [19]) for 48 h prior to GSIS assays. Details of donors of pancreatic islets treated with EPDR1 protein are shown in Table S2. For *Epdr1* silencing, INS1 832/13 cells (1.7×10^5 cells/cm^2) were seeded in 24 well plates and transfected after 24 h with 10 nM of scramble negative control (NC) (Thermofisher, custom select siRNA: 5′- GAGACCCUAUCCGUGAUUAUU-3′) or rat *Epdr1* siRNA (Thermofisher, #4390771; s145532). EndoC-βH1 cells (1.5×10^5 cells/cm^2) were seeded in 48 well plates and transfected 24 and 48 h after (two successive days, double shot) with 40 nM of Silencer Select Negative Control No. 1 siRNA (Thermofisher, #4390843) or human *EPDR1* siRNA (Thermofisher, # 4392420; s29379). Human pancreatic islets (400–500) were seeded in 35 mm petri dish containing 2 mL of RPMI medium (5 mM glucose, 10% FBS (Sigma #7524), 200 mM L-Glutamine) and transfected on two successive days with 0.5 mL of 50 nM of a Silencer Select Negative Control No. 1 siRNA (Thermofisher, #4390843) and human *EPDR1* siRNA (Thermofisher, #4390771; s29379), using Lipofectamine RNAiMAX Transfection Reagent (Thermofisher, #13778075). Details of donors of pancreatic islets used for experiments of *EPDR1* silencing are given in Table S3. Human pancreatic islets were cultured as previously described [24]. All procedures were approved by appropriate Swedish Ethical Committees.

2.5. mRNA analysis

Total RNA was extracted using the RNeasy Mini Kit (Qiagen) and cDNA was generated with the RevertAid First-Strand cDNA synthesis kit. 10 ng cDNA/well (in duplicates) were used for qPCR (*Epdr1* rat (Rn01525240_m1) and human (Hs01556067_m1) taqman assay were obtained from Thermofisher). qPCR assays were performed using the Applied Biosystems QuantStudio7 Flex Real-Time PCR System (Thermofisher). Relative gene abundance was calculated using the $\Delta\Delta$Ct method with β-*actin* as housekeeping reference gene and expressed as fold change to control.

2.6. Secreted lactate measurement

INS1 832/13 cells (1.7×10^5 cells/cm^2) were seeded in 24 well plates, transfected with scramble (negative control, NC) or *Epdr1* siRNA (10 nM) (as described in section 2.3) and GSIS determined (as

described in section 2.2). The concentration of the extracellular lactate accumulated during 1 h in response to stimulation with SAB buffer with LG and HG glucose was measured by use of the Lactate Colorimetric/Fluorometric Assay Kit (Biovision, #607-100) following the manufacturer's instructions. Briefly, cell conditioned samples and lactate standards were mixed with an enzyme plus fluorescent probe mix in a ratio 1:1, incubated for 30 min (at room temperature) and Fluorescence emission read (Ex/Em = 535/590 nm) in a microplate reader. Lactate concentrations were normalized by total cell mass in respective wells (protein mass measured by Pierce BCA Protein Assay Kit).

2.7. Metabolomics analysis

The cellular metabolome was analyzed by combined gas chromatography-mass spectrometry (GC-MS) as previously described [25]. Briefly, INS1 832/13 cells were stimulated with SAB LG, HG or HG + IBMX for 1 h (as described for GSIS above) and total cell metabolites extracted with methanol/water (9/1, v/v) containing a cocktail of stable isotope labelled internal standards ($^{2}H_4$-succinate (0.22 mg/L), $^{2}H_8$-valine (4.41 mg/L), $^{13}C_4$-3-hydroxybutyric acid (2.21 mg/L), $^{13}C_5{}^{15}N$-glutamic acid (22.06 mg/L), $^{2}H_{19}$-decanoic acid (4.41 mg/L) and $^{2}H_{31}$-palmitic acid (22.06 mg/L). Proteins were precipitated by three repeated rounds of shaking/snap freezing on liquid nitrogen, incubation in ice for 1 h and centrifugation. Seven independent experiments were performed.

The generated raw data were pre-processed using an in-house script developed at Swedish Metabolomics Centre, Umeå, Sweden. The detected peaks were identified by comparison of mass spectra and retention indexes using NIST MS Search v.2.0, using in-house and NIST98 spectral databases. After pre-processing and filtering of the metabolites of high coefficient of variation in quality control pool samples (>25%), levels of 21 metabolites were used for further analysis.

2.8. Mitochondrial oxygen consumption (OCR) measurements

OCR was evaluated with an XFe24 extracellular flux analyzer. INS1 832/13 cells were transfected with scramble (negative control, NC) or *Epdr1* siRNA (10 nM) and cultured for 72 h. Cells were starved in SAB LG (2.8 mM) for 2 h and OCR was measured in SAB (without bicarbonate/HEPES) every 3 min for 90 min. OCR was measured at basal glucose (2.8 mM glucose) and after adding HG (16.7 mM), 5 μM oligomycin, 4 μM Carbonyl cyanide p-trifluoromethoxyphenylhydrazone (FCCP), and 1 μM rotenone/antimycin A. Wave Seahorse Software and an online tool (seahorseanalytics.agilent.com) were used to analyze data. Non-mitochondrial respiration was subtracted, and OCR data normalized to total protein content, determined by the colorimetric Biuret method (Pierce-BCA Protein Assay Kit, Thermofisher).

2.9. Immunoblot analysis

INS1 832/13 cells (1.7×10^5 cells/cm^2) were seeded in 24 well plates, transfected with scramble (negative control, NC) or *Epdr1* siRNA (10 nM) (as described in section 2.3) and 72 h later cells were washed with cold PBS and cells lysed with RIPA buffer (containing complete protease inhibitor cocktail). Protein concentration was measured by Pierce BCA Protein Assay Kit and 30 μg of total protein electrophoresed on 4–15% mini-Protean TGX precast gel (Bio-Rad), transferred onto a PVDF membrane (Bio-Rad) and blocked with BSA 5.0% in TBST (Tris-buffered saline+0.1% Tween 20 for 1 h at room temperature. Next, the membranes were incubated overnight with Total OXPHOS Rodent WB Antibody Cocktail (abcam, #ab110413) diluted 1:250 in TBST-BSA 2%. Horseradish-peroxidase-linked goat anti-mouse IgG (1:3000 dilution (Biorad, #1706516) was used as a secondary antibody. Blots were developed with enhanced chemiluminescence (ECL). Densitometry analysis was performed using BioRad ImageLab software and total protein load (stain free) was used as a loading control.

2.10. Cytosolic ATP/ADP-ratio

Single cell cytosolic ATP/ADP-ratio measurements were performed using the genetically encoded biosensor PercevalHR [26] and pHrodo Red AM intracellular pH indicator (c: p35372, Life Technologies). Cells were co-transfected with NC or *Epdr1* siRNA (10 nM) and 1 μg PercevalHR plasmid (c:49083, Addgene). Cells were starved for 2 h in SAB LG and preincubated for 1 h with pHrodo Red AM (diluted 1/1,000). PercevalHR fluorescence was recorded by laser excitation/emission at 490/530 nm and normalized to the pHrodo Red AM fluorescence emission recorded at 560/585 nm on a Zeiss LSM510 confocal microscope for 30 min/well (scan time of 7.86 s).

2.11. Quantification of whole-cell ATP and ADP

Cellular ATP and ADP levels were quantified by ultra-high performance liquid chromatography-tandem mass spectrometry (UHPLC-MS/MS). Prior to analysis, the cell extracts were diluted 10 times with MeOH/water (1/1, v/v) with final concentration of the labelled internal standards (AMP-$^{13}C_{10}{}^{15}N_5$, ADP-$^{15}N_5$, ATP-$^{13}C_{10}$) of 1 μM. Separation of the nucleotides was achieved with a 15-minute gradient using a iHILIC-(P) Classic column (PEEK, 50 × 2.1 mm, 5 μm, HILICON, Umeå, Sweden) with mobile phases composed of (A) 10 mM ammonium acetate in water at pH 9.4 and (B) 10 mM ammonium acetate at pH 9.4 in 90% acetonitrile, both mobile phases were supplemented with 5 μM medronic acid. The flow rate was 0.35 mL/min, and the gradient elution program was set as follows: 0.0 min (85% B), 5 min (60% B), 7 min (30% B), 8 min (30% B), 9 min (85% B), and 15 min (85% B). The UHPLC-MS/MS system consisted of an Agilent 1290 UPLC connected to an Agilent 6490 triple quadrupole tandem mass spectrometer (Agilent, CA, USA). Analytes were ionized using electrospray ionization operated in positive ionization mode. The source and gas parameters were set as follows: ion spray voltage 4.0 kV, gas temperature 150 °C, drying gas flow 11 L/min, nebulizer pressure 20 psi, sheath gas temperature 325 °C, sheath gas flow rate 12 L/min, fragmentor 380 V. Multiple reaction monitoring (MRM) transitions for AMP, ADP, ATP, and their respective labelled internal standards were optimized by flow injection analysis. Quantification of AMP, ADP, and ATP was conducted based on internal standard calibration. Calibration curves were linear from 5 nM to 50 μM. The accuracy, determined through spiking experiments of the cell extracts (n = 4) with 10 μM standards, was within the acceptable range of 100 ± 15%.

2.12. Statistical analysis

Data are shown as mean ± SEM of at least three independent experiments. The Student's t test was used to compare two groups and ANOVA for multiple groups. Statistical significance was set at $p < 0.05$. SPSS 28 and Prism 9.0 (GraphPad) were used for statistical analysis and graph generation. Batch effects were removed from metabolomics data using ComBat [27] and data expressed as fold change of each metabolite in HG and HG + IBMX relative to LG simulated cells. ANOVA was applied for identifying differentiating metabolites between two genotypes and p values were corrected for multiple testing with the Benjamini–Hochberg procedure. Prior to multivariate analysis, data was mean-centered and scaled to unit variance to ensure equal weight of all metabolites in analysis. Unsupervised principal component analysis (PCA) was first used to recognize underlying patterns and to detect outliers. Supervised orthogonal

partial least-squares discriminant analysis (OPLS-DA) was then performed to find discriminating metabolites based on the variable importance on projection (VIP) score. The VIP measures the influence of metabolites on the predictive component in the model, in other words; how much influence the metabolite has on discriminating the two different genotypes (*Epdr1*-KD vs NC control). Metabolites with VIP score >1 were considered metabolites responsible for the separation between the two genotypes. The OPLS-DA model was validated with 3-fold cross-validation and permutation test ($n = 200$) (Figure S1). All the metabolomics analysis was carried out in R 4.1.2. Pathway enrichment analysis was performed with MetaboAnalyst based on the Kyoto Encyclopedia of Genes and Genomes (KEGG) library using hypergeometric test.

3. RESULTS

3.1. *EPDR1* mRNA levels in human islets are upregulated in T2D and obese subjects and correlated to GSIS *ex vivo*

We first investigated whether *EPDR1* mRNA expression in human pancreatic islets was affected by metabolic (obese vs normo-weight), glycaemic (HbA1c) and disease status (T2D vs. non-diabetic (ND)) (Figure 1). We observed that *EPDR1* mRNA levels were significantly elevated in islets from T2D vs ND (Figure 1A) and from overweight/obese (BMI >27 kg/m^2) vs normo-weight donors (BMI <27 kg/m^2) (Figure 1B). Similarly, a suggestive increase of *EPDR1* mRNA levels in islets from T2D vs ND donors and their positive correlation with donors BMI was found when the expression was tested by qPCR in a small subset of donors (Figure S2A and B). To gain insight into a potential role of EPDR1 in human islet function and glucose homeostasis, we evaluated the association between islet *EPDR1* mRNA levels and glycemic control (HbA1c) and GSIS *ex vivo*; the data were analysed separated by disease status (Figure 1C–G). In pancreatic islets from ND donors, we found that *EPDR1* mRNA levels were positively correlated with BMI (Figure 1C), HbA1c (Figure 1D), and GSIS (Figure 1E). In contrast, in pancreatic islets from T2D donors, we observed a negative correlation between *EPDR1* mRNA levels and HbA1c (Figure 1F) but a strong positive correlation with GSIS (Figure 1G). These data indicate that *EPDR1* mRNA levels are upregulated under metabolic stress conditions (hyperglycaemia/obesity) and associated with increased GSIS. This could be viewed as a compensatory mechanism to improve β-cell function, resulting in insulin hypersecretion to maintain glucose homeostasis in the context of insulin resistance of obese subjects.

3.2. *EPDR1* eQTLs are associated with functional outcomes of human islets

To explore whether genetic variance could affect *EPDR1* gene expression in human pancreatic islets, we first looked up genome-wide significant expression quantitative trait loci (eQTL) for *EPDR1* in the Inspire cohort with data from 420 donors [28]. We found loci with genome-wide significant associations to *EPDR1* expression in human islets (rs6965395 and rs1524054) and others that were borderline significant (rs4720265, rs3734952, rs10488617 and rs3213975 with nominal p-values $= 2.5 \times 10^{-21}$, 7.14×10^{-21}, 4.5×10^{-22}, 4.5×10^{-22}, respectively). Next, we assessed whether these SNPs were also eQTLs in sorted human β-cells in the Inspire cohort. We found that the SNP rs6965395 was significantly associated with *EPDR1* expression in sorted β-cells (nominal p-value $= 1.69 \times 10^{-17}$).

Next, we evaluated whether the *EPDR1* eQTLs found in the Inspire cohort could be replicated in our human pancreatic islet cohort (188 donors-EXODIAB [21]) and whether it could translate into β-cell functional outcomes. Linear models were built to assess the association between *EPDR1* genotypes in these SNPs (rs4720265, rs3734952, rs10488617 and rs3213975) and gene expression (Figure 2A–D). Age, BMI, purity and days of culture were set as covariates. We confirmed that carriers of the alternative allele for all these SNPs had reduced *EPDR1* gene expression in pancreatic islets (Figure 2A–D). Interestingly, genotypes of these eQTLs had suggestive association with parameters of β-cell function, with carriers of the minor allele and lower *EPDR1* mRNA levels, showing reduced GSIS stimulatory index (Figure 2E–H) and GLP1-promoted GSIS (Figure 2I–L). These data indicate that *EPDR1* eQTLs in human islets could potentially affect human β-cell function, via changes in *EPDR1* expression.

3.3. EPDR1 positively regulates GSIS in human β-cells

To evaluate the potential regulation of human β-cell function by EPDR1, the effect of silencing *EPDR1* expression and of treatment with the recombinant human EPDR1 protein [19] on GSIS was tested in pancreatic islets obtained from ND donors and in the human EndoC-βH1 β-cell line (Figures 3 and S2). Reduced expression of *EPDR1* in human islets transfected with *EPDR1* vs scramble (control) siRNA was confirmed by qPCR analysis (Figure 3A). GLP1R is a Gαs-protein-coupled receptor and acts by increasing cAMP accumulation and activation of signaling pathways mediated by PKA and Epac [29]. Thus, to mimic GLP1R activation, IBMX was used to increase the accumulation of cAMP.

As expected, a clear increase in insulin secretion in response to glucose and glucose + IBMX was observed in the control human islets (Figure 3B). However, insulin secretion in response to glucose was significantly reduced upon *EPDR1* silencing in human islets (Figure 3B). The effect of *EPDR1* silencing on GSIS was also tested in EndoC-βH1 β-cells; no significant changes were observed (Figure S3), which may be explained by the low endogenous *EPDR1* mRNA expression level in EndoC-βH1 β-cells (Figure S2A), a potential consequence of their fetal genomic signature [30].

Next, human islets from ND donors were treated with vehicle or increasing concentrations of human EPDR1 protein for 48 h and insulin secreted in response to stimulation with glucose or glucose + IBMX was measured. No significant changes were observed in insulin secretion at basal, high glucose and glucose + IBMX conditions in response to EPDR1 vs vehicle treatment (Figure 3C). To overcome the potential obstacle of EPDR1 protein to reach β-cells within the pancreatic islet core or any confounding effects of islet non-β-cells (secretion of other islet hormones), human EndoC-βH1 β-cells were also treated with same human EPDR1 protein concentrations and insulin secretion in response to glucose stimulation measured. Treatment of EndoC-βH1 β-cells with human EPDR1 protein resulted in significantly increased GSIS (Figure 3D). Overall, the data described here indicate that human EPDR1 protein is positively regulating human β-cell function by increasing glucose-responsiveness and insulin secretion.

3.4. EPDR1 is required for glucose- and pyruvate- but not K^+-stimulated insulin secretion in β-cells

To evaluate whether the role of EPDR1 in β-cells is conserved among different species and to deepen our knowledge about the molecular mechanisms of EPDR1 in β-cell function, we examined the EPDR1 actions on INS1 832/13 cells, a well characterized glucose-responsive clonal rat β-cell line [22]. *Epdr1* was silenced by transfection of *Epdr1* siRNA and reduced *Epdr1* expression confirmed by qPCR (Figure 4A). Then, the effects of silencing *Epdr1* on insulin secretion in response to different metabolic and pharmacologic stimuli were assessed (Figure 4B–E).

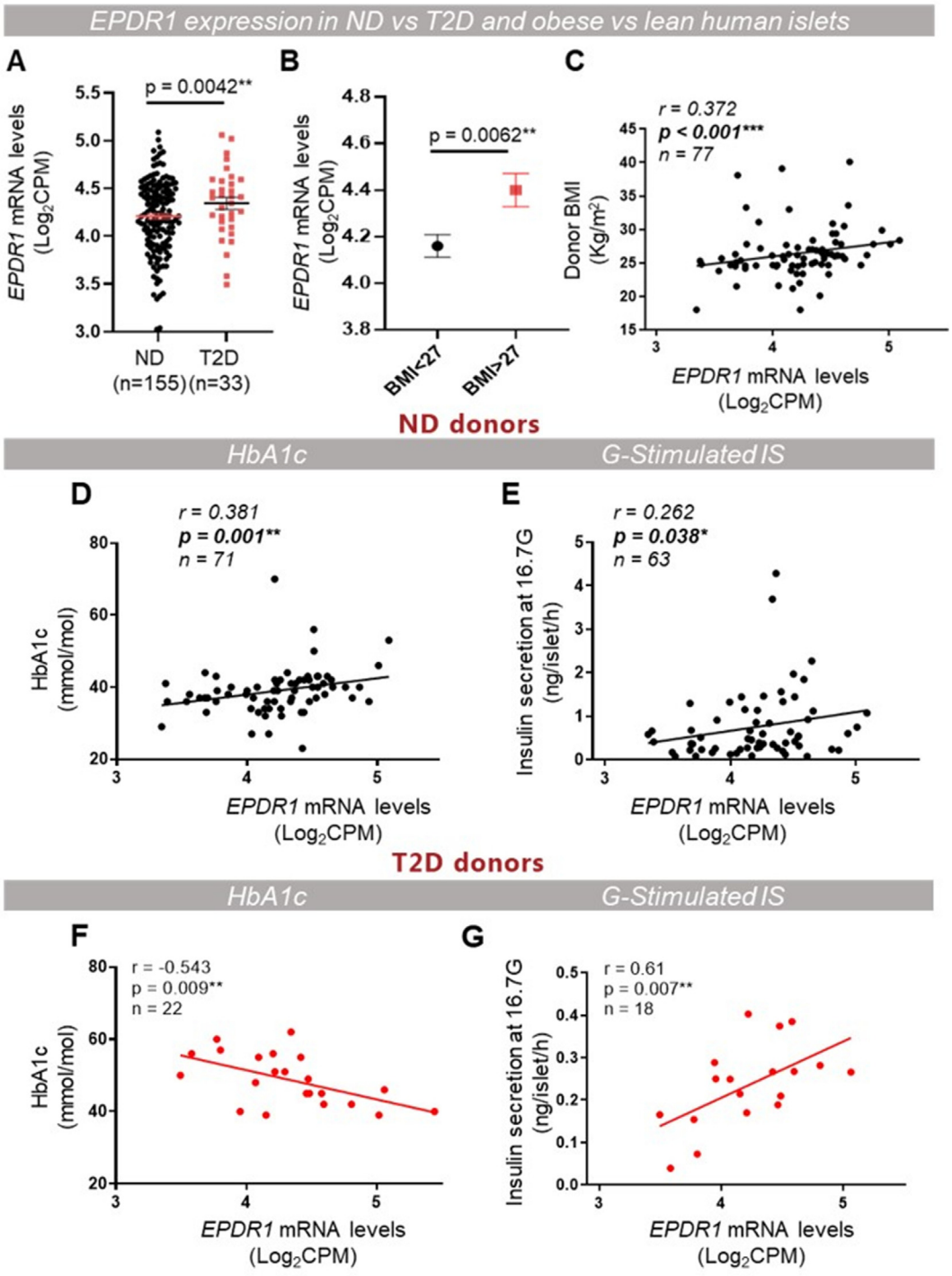

Figure 1: *EPDR1* mRNA levels in human islets are upregulated in T2D and obese donors and are associated with *ex vivo* GSIS. (A) *EPDR1* mRNA in ND (n = 160) vs T2D (n = 35) islets and (B) in normo-weight (BMI<27; n = 67) and overweigh/obese (BMI>27; n = 33) donors, *p < 0.05, **p < 0.01 by unpaired student's t-test. Rank–Spearman correlation analysis between *EPDR1* mRNA levels and (C) Donor BMI, (D) HbA1c, and (E) GSIS in ND donor islets. Rank–Spearman correlation analysis between *EPDR1* mRNA levels and (F) HbA1c and (G) GSIS in T2D donor islets.

Silencing of *Epdr1* expression resulted in significantly reduced insulin secretion in response to stimulation with glucose and pyruvate but not with the plasma membrane depolarizing agent KCl (Figure 4B). These data suggest that EPDR1-increased GSIS is mediated by changes on mitochondrial metabolism of glycolysis-derived pyruvate but may leave other processes such as insulin production, β-cell mass or the exocytosis machinery unaffected.

INS1 832/13 cells are poorly responsive to GLP1 or GLP1R agonist such as Exendin-4 [22]. Thus, to mimic GLP1R activation, IBMX and forskolin (FSK) were used to trigger cAMP/PKA/Epac signalling. As

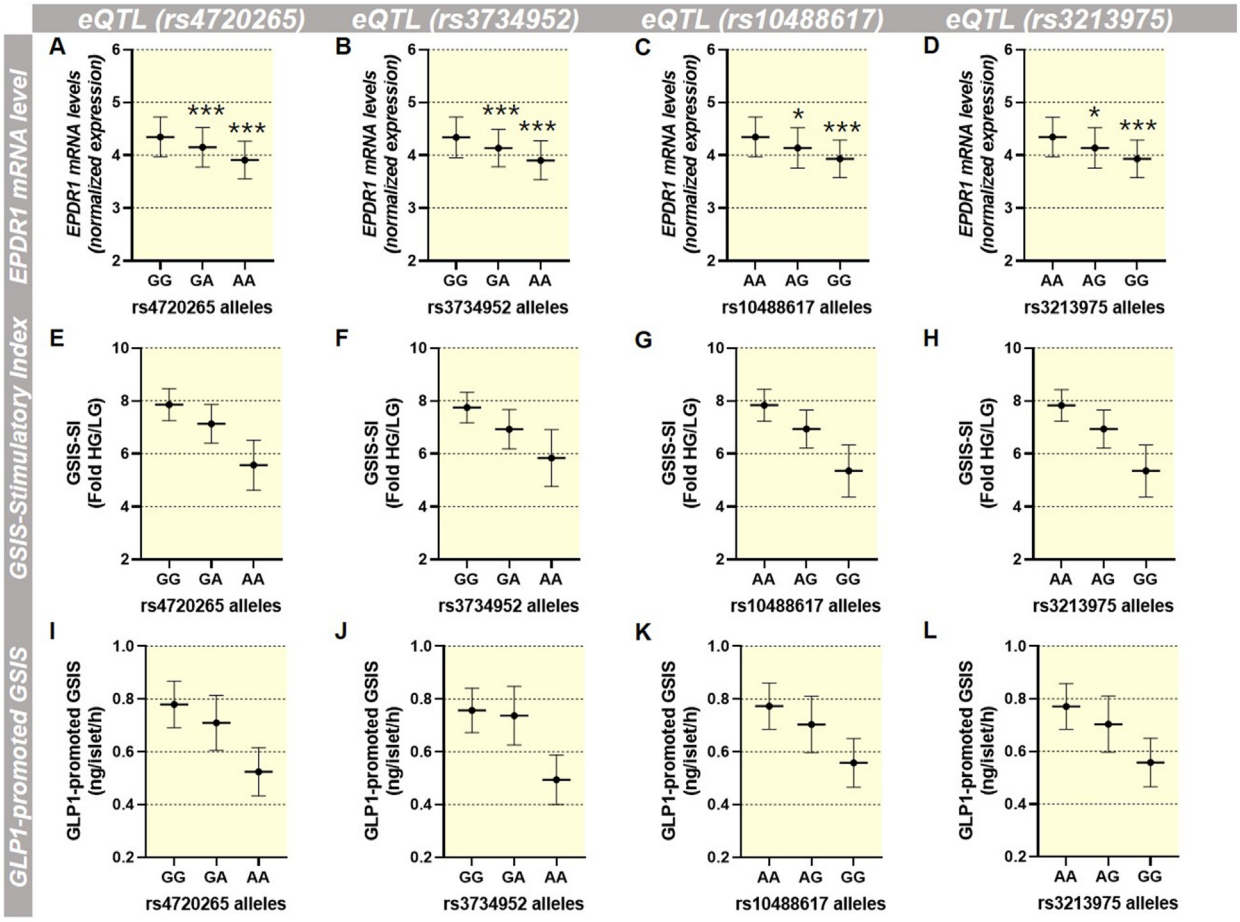

Figure 2: *EPDR1* eQTLs are associated with functional outcomes of human islets. The alleles (GG-GA-AA) of SNPs; rs4720265, rs3734952, rs10488617 and rs3213975 are associated with: (A—D) *EPDR1* mRNA levels, (E—H) GSIS-Stimulatory Index and, (I—L) GLP1-promoted GSIS in human pancreatic islets. Linear regression analysis for the SNPs alleles (eQTLs) vs. *EPDR1* mRNA levels was performed adjusting by the next covariates; age, BMI, T2D, purity (%) and days in culture of isolated islets. For the relation between the *EPDR1* SNPs alleles and the functional variables one-way ANOVA was performed. *$p < 0.05$, ***$p < 0.001$.

expected, IBMX and FSK amplified GSIS in control cells and this effect was significantly reduced in the *Epdr1*-KD cells (Figure 4C).

The harmful effects that chronic high glucose and free fatty acids exert on β-cell metabolism and function are well described [3,31]. To further explore the metabolic mechanisms of EPDR1-regulated GSIS, *Epdr1*-KD and control INS1 832/13 cells were exposed to high glucose (20 mM) or palmitate (0.5 mM) for 24 h (mimicking mild glucotoxic or lipotoxic conditions). The deleterious effects of high glucose and high palmitate *in vitro* in control cells were confirmed as they reduced the average stimulatory index (fold change of insulin secretion in response to high vs. low glucose stimulation) from 10.3 to 3.5 and 5.0, respectively (Figure 4D). Interestingly, *Epdr1* silencing resulted in reduced GSIS in the control (normo-glucose) and high palmitate conditions but not at high glucose (Figure 4D). Considering that the glucotoxic effects on β-cells are driven by chronically elevated mitochondrial glucose metabolism [3], our results support the idea that EPDR1 is positively regulating GSIS by promoting mitochondrial glucose metabolism in β-cells.

Finally, to confirm the positive effects of EPDR1 on β-cell function observed in human islets and EndoC-βH1 β-cells (Figure 3C and D), INS1 832/13 cells were long-term treated with human EPDR1 protein and GSIS measured. GSIS was significantly increased in response to treatment with the EPDR1 protein (Figure 4E), indicating that EPDR1 protein positively regulates β-cell function.

3.5. EPDR1 is not required for glucose promoted cytosolic calcium oscillation in β-cell

To explore potential molecular mechanisms underlying the positive effects of EPDR1 on GSIS, we first performed experiments using the calcium sensor dye (Fluo4-AM) and confocal microscopy to evaluate single cell cytosolic calcium response to glucose or pyruvate stimulation in control (NC) and *Epdr1*-KD INS1 832/13 cells (Figure S4). In control cells, cytosolic calcium increased in response to glucose (Figure S4A—D) and pyruvate (Figure S4E—H) stimulation and acutely spiked in response to KCl (plasma membrane depolarization). This confirms that INS1 832/13 cells were responsive to metabolic and electrochemical signals that converge into plasma membrane depolarization, opening of VDCC and calcium uptake. However, there was no differences in the cytosolic calcium responses to glucose or pyruvate in NC vs *Epdr1*-KD cells when the average AUC (Figure S4B and F) or the average oscillation frequency (Fig. S4D and H) was compared. These data indicate that the EPDR1 mode of action is not mediated by changes in calcium uptake or buffering cytosolic calcium (into ER or mitochondria) in response to glucose or pyruvate. Instead, the mode of action is likely downstream of glucose-induced cytosolic calcium influx.

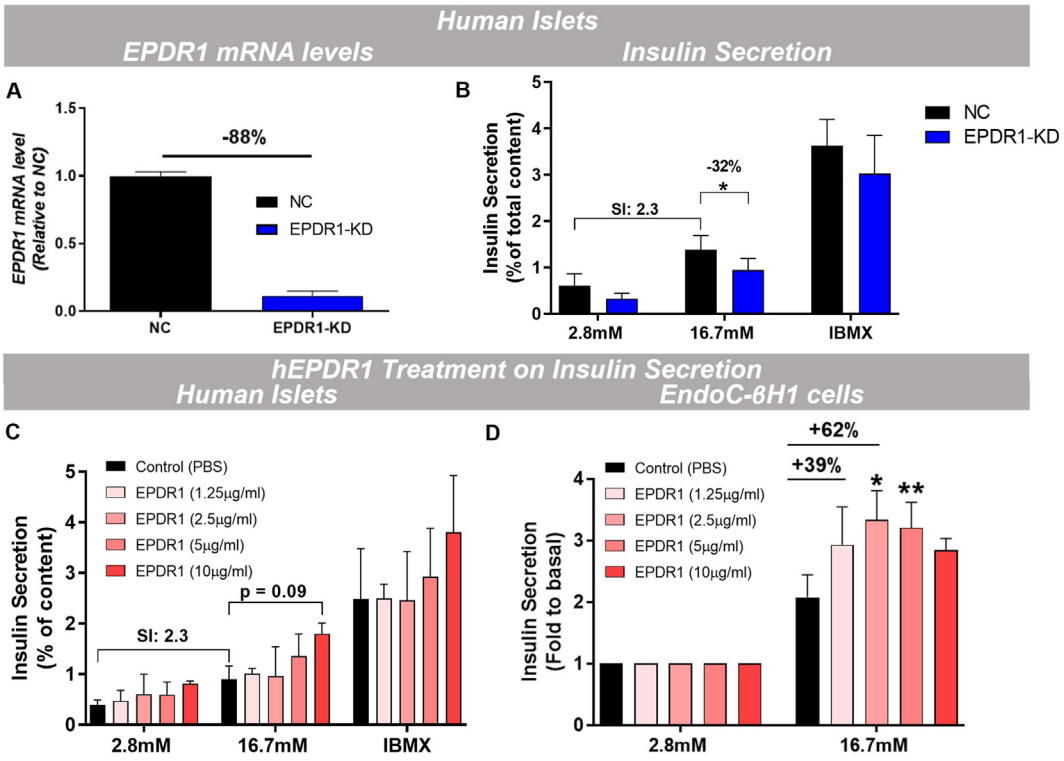

Figure 3: EPDR1 increases GSIS in human islets. Pancreatic islets from ND donors were transfected with a scramble (negative control-NC) siRNA or *EPDR1* siRNA (50 nM - *EPDR1*-KD) in two successive days, 72 h after the first transfection; (A) *EPDR1* mRNA levels in *EPDR1*-KD and NC control human islets were analysed by qPCR (n = 4), (B) Insulin secretion in response to stimulation with SAB low (2.8 mM), high glucose (16.7) or high glucose + IBMX (100 µM) for 1 h in *EPDR1*-KD vs NC control human islets, data are expressed as % of insulin secreted from total insulin content (n = 4). (C) Pancreatic islets from ND donors were treated for 48 h with recombinant human EPDR1 protein in various doses (1.25–10 µg/ml) and insulin secretion in response to stimulation with SAB low (2.8 mM), high glucose (16.7) or high glucose + IBMX (100 µM) for 1 h measured (n = 3). (D) EndoC-βH1 cells were treated for 48 h with recombinant human EPDR1 protein in various doses (1.25–10 µg/mL) and the insulin secretion in response to stimulation with SAB low (2.8 mM) and high glucose (16.7) for 1 h measured (n = 3). For Figures C and D, the statistical analysis compared the levels of insulin secretion in response to glucose in cells treated with each dose of EPDR1 vs vehicle. Graph bars represent mean ± SEM. *p < 0.05, **p < 0.01 by paired student's t-test.

3.6. Metabolomics analyses suggest that EPDR1 is required for coupling glycolytic to mitochondrial metabolism

To further investigate the molecular mechanism by which EPDR1 positively regulates GSIS, mass-spectrometry-based metabolomics analysis in response to glucose stimulation in NC and *Epdr1*-KD INS1 832/13 cells was performed (Figure 5). PCA and OPLS-DA were used to find the set of metabolite changes in response to glucose (fold change HG/LG after 60 min of stimulation) that best explained the variance between NC and *Epdr1*-KD cells (Figure 5A and B). Based on the VIP for metabolites, namely, a score of the power each metabolite has to influence the discrimination of genotypes (*Epdr1*-KD vs NC control), metabolic pathway analysis (over-representation analysis tests) was performed (Figure 5C). Remarkably, metabolic pathways critical for GSIS such as the Warburg effect, the malate-aspartate shuttle and the TCA cycle were significantly over-represented (Figure 5C) and may explain the molecular mechanism by which EPDR1 regulate GSIS in β-cells.

Relative changes in cell metabolite levels in response to glucose for each of these metabolic pathways were further analysed (Figure 5D,E, G, and H). The data indicated that *Epdr1* silencing results in decreased levels of pyruvate, but increased levels of lactate (Figure 5D) and the lactate/pyruvate-ratio (Figure 5E); this suggests diversion of glycolysis-derived pyruvate from mitochondrial metabolism to lactate production (Warburg effect). Consequently, we quantified (via an enzymatic method) the secreted lactate accumulated (in SAB conditioned medium) during 1 h of glucose stimulation in the control (NC) and *Epdr1*-KD cells and found a 38% higher concentration of lactate in the *Epdr1*-KD compared to the NC control cells (Figure 5F); this may reflect a deviation of pyruvate from the TCA cycle to lactate production in the *Epdr1*-deficient β-cells. In addition, in the *Epdr1*-KD cells, the glucose responsiveness of several TCA cycle metabolites, such as citrate, isocitrate, α-ketoglutarate (AKGA), succinate and malate were reduced while the glucose-provoked reduction in aspartate levels was also decreased (Figure 5G andH). Likewise, the citrate/pyruvate- and AKGA/pyruvate-ratios were strongly reduced in the *Epdr1*-KD vs NC control cells, indicating reduced entrance of pyruvate into the mitochondrial TCA cycle or, alternatively, reduced TCA cycle anaplerosis/increased cataplerosis (Figure 5G and H). In line with the metabolic pathway analysis, increased aspartate (less reduced) and reduced malate levels in response to glucose in the *Epdr1*-KD vs NC control cells (Figure 5G and H) suggested altered activity of the malate-aspartate-shuttle. This may lead to reduced anaplerosis and reduced replenishment of cytosolic NAD^+, which may also contribute to uncoupling glycolysis and mitochondrial metabolism. In line with this, a compensatory increase in lactate production is observed, which may serve to maintain glycolytic flux (upon replenishing the cytosolic NAD^+). Overall, the metabolic changes observed in *Epdr1*-KD vs NC control cells were compatible with a model where the glycolysis-derived pyruvate is diverted from mitochondria to production of lactate.

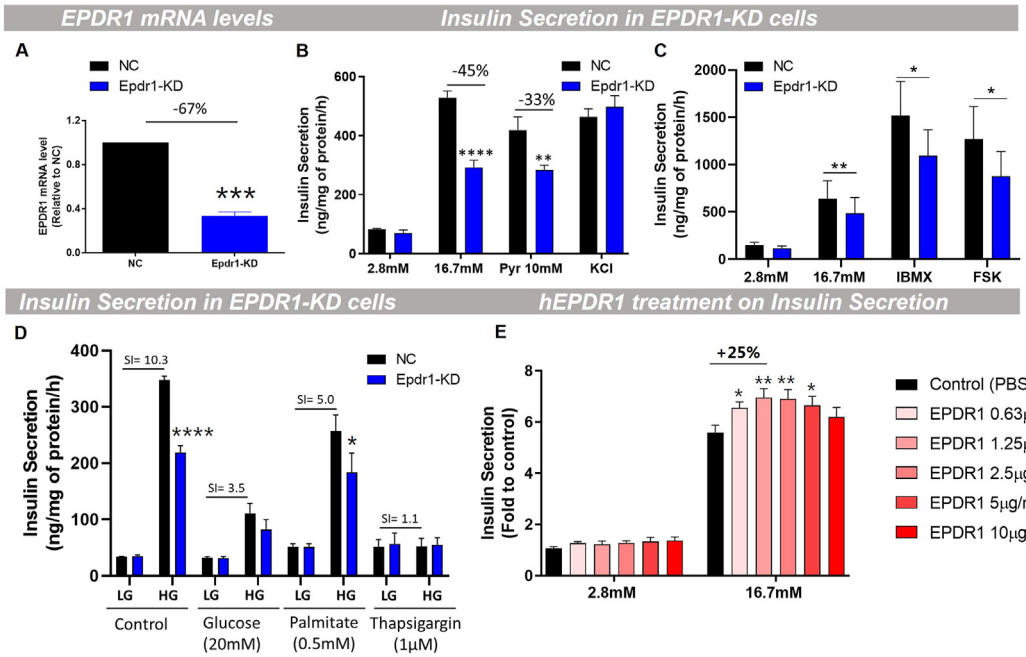

Figure 4: EPDR1 is required for glucose- and pyruvate- but not KCl-stimulated insulin secretion in β-cells. A-D) INS1 832/13 cells were transfected with NC scramble or *Epdr1* siRNA (10 nM) for 72 h. (A) mRNA levels in *Epdr1*-KD vs NC control cells. (B) Insulin secretion in response to low (2.8 mM), high glucose (16.7), Pyruvate (10 mM) or KCl (30 mM) in *Epdr1*-KD vs NC control cells (n = 4). (C) Insulin secretion in response to low (2.8 mM), high glucose (16.7), high glucose + IBMX (100 μM) or high glucose + FSK (10 μM) in *Epdr1*-KD vs NC control cells (n = 6). (D) Insulin secretion in response to low (2.8 mM) or high glucose (16.7) in *Epdr1*-KD vs NC INS1 832/13 cells treated with high glucose (20 mM), high palmitic acid (0.5 mM) or Thapsigargin (1 μM) for 24 h (n = 4). (E) Insulin secretion in response to low (2.8 mM) or high glucose (16.7) INS1 832/13 cells treated with human EPDR1 protein (0.63—10 μg/ml) (n = 4). Graph bars represent mean ± SEM. *p < 0.05, **p < 0.01, ***p < 0.001, ****p < 0.0001 by paired student's t-test and two-way ANOVA accordingly.

An essential role of the malate-aspartate shuttle for the incretin-induced amplification of GSIS has been reported [32]. Thus, similar metabolomics analysis were also applied in response to glucose + IBMX stimulation in *Epdr1*-KD vs NC INS1 832/13 cells (Figure S5). In line with the notion that *Epdr1* silencing results in defective mitochondrial metabolism, the Warburg effect, the malate-aspartate shuttle and the TCA cycle also came up as significant metabolic pathways explaining the differences between *Epdr1*-KD vs NC control INS1 832/13 cells in response to glucose + IBMX stimulation (Figure S5D). Univariate analyses confirmed an increase of the lactate and lactate/pyruvate ratio (Warburg effect) and reduced TCA cycle metabolite levels in the *Epdr1*-KD vs NC control cells in response to glucose + IBMX stimulation (Figure S5E—G). Therefore, our data suggested that EPDR1 is increasing GSIS by directing the metabolism of glycolysis-derived pyruvate through the mitochondrial TCA cycle.

3.7. EPDR1 is required for the glucose-stimulated increases of the cytosolic ATP/ADP-ratio

To deepen our understanding of the mechanisms of EPDR1 in regulating glucose-stimulated mitochondrial metabolism and insulin secretion, we measured mitochondrial oxygen consumption rate (OCR) in response to glucose in the *Epdr1*-KD and NC control INS1 832/13 cells (Figure 6). We observed a slight but significant decrease in the acute OCR response to glucose (Figure 6B) in response to glucose in the *Epdr1*-KD and NC control INS1 832/13 cells. No significant changes in mitochondrial ATP-linked OCR ($p = 0.090$, Figure 6C), the mitochondrial proton-leak or maximal OCR were observed (Figure 6D and E). We also tested the expression level of representative protein of mitochondrial Electron Transport Chain (ETC) Complexes (I—V). Interestingly, significantly increased levels of SDHB protein of complex II was found in *Epdr1*-KD vs NC control INS1 (832/13) cells (Figure S6).

To further investigate the bioenergetic alteration caused by *Epdr1*-deficiency in INS1 832/13 cells, single cell cytosolic ATP/ADP-ratio was measured using the genetically encoded PercevalHR biosensor [26] (Figure 6F and G). As expected for glucose-responsive β-cells, the cytosolic ATP/ADP-ratio in control cells was increased in response to glucose but this was blunted in the *Epdr1*-KD cells (Figure 6F and G). To confirm this finding, whole-cell adenine nucleotide content in response to glucose stimulation (1 h) was measured by mass spectrometry and the whole-cell ATP/ADP-ratio calculated in the *Epdr1*-KD vs NC control cells (Figure 6H—J). As expected, levels of ADP decreased in control cells (Figure 6H) while those of ATP slightly increased (Figure 6I). Consequently, the ATP/ADP-ratio increased about 15 times (fold change in HG vs LG. Figure 6J) after 1 h of glucose stimulation. Remarkably, in the *Epdr1*-KD cells, the glucose-elicited rise in the ATP/ADP-ratio was blunted (Figure 6J). Thus, these data support the idea that EPDR1 is required for coupling of glycolysis and TCA cycle metabolism in β-cells.

4. DISCUSSION

Previous reports have described a relationship between EPDR1 expression and tumor progression/prognosis in different types of cancers [7,33,34]. Although it is known that metabolic reprograming occurs in tumor cells, no obvious clues about the biological role of EPDR1 have been inferred.

Progress regarding this was recently reached by two studies: one revealing the crystal structure of human EPDR1 [35], and the other

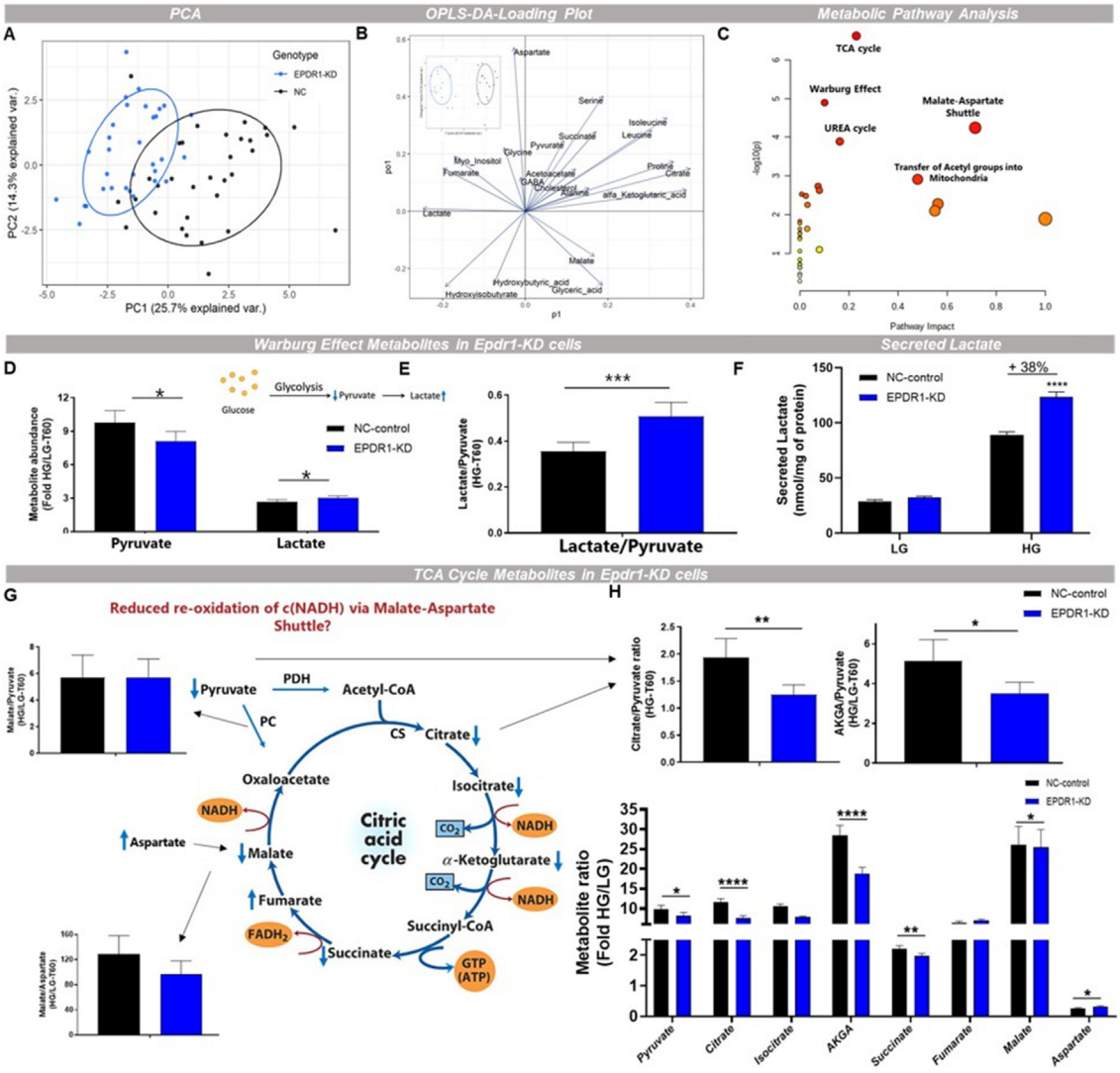

Figure 5: Metabolomics analysis in cells stimulated by glucose indicates that EPDR1 tightens the glycolysis-mitochondrial metabolism coupling. Metabolomics analysis after 1 h of glucose (HG) stimulation in NC and *Epdr1*-KD INS1 832/13 cells (n = 7). (A) PCA for metabolites levels at HG/LG, (B) OPLS-DA loading scatter plot; it describes the relationship between a metabolite and the specific component, the absolute value of the loading indicates how much the metabolite influences the specific component whereas the sign of the loading indicates whether the influence is positive or negative on this component. Horizontal axis shows X-loadings p and the Y-loadings q of the predictive component (pq1). The vertical axis showing the X-loading p(o) and the Y-loadings s(o) for the Y-orthogonal component (poso1). Inserted in the Figure is the Supervised orthogonal partial least-squares discriminant analysis (OPLS-DA) score plot, showing the predictive (t1) and 1st orthogonal component (to1). (C) Metabolic Pathway Analysis using the predictive component (VIP) of the OPLS-DA model, showing the metabolic pathways that explain the variance between *Epdr1*-KD vs. NC control cells. (D) Mass spectrometry measured cellular metabolites abundance in response to glucose (fold change HG/LG) of pyruvate and lactate. (E) Ratio of cellular abundance of Lactate/Pyruvate. (F) Secreted extracellular lactate concentration during GSIS (1 h) in NC and *Epdr1*-KD INS1 832/13 cells (n = 4). (G) TCA cycle scheme. (H) Mass spectrometry measured cellular metabolites abundance in response to glucose (fold change HG/LG) showing differences of TCA cycle and malate/aspartate shuttle metabolites such as; reduced citrate and alpha-ketoglutarate (AKGA) and increased aspartate in *Epdr1*-KD vs NC control cells. Data are mean ± SEM of n = 7 independent experiments. *p < 0.05; **p < 0.01; ***p < 0.001; ****p < 0.0001 with Combat batch correction method followed by ANOVA on genotype.

identifying EDPR1 as a secreted human batokine [19]. Thus, EPDR1 influences the expression of mitochondrial proteins and the NE-stimulated mitochondrial proton-leak respiration associated with thermogenesis in hBAT [19]. Moreover, it was recently shown that EPDR1 regulates osteoblast metabolism and maturation [36]. Thus, EPDR1 may also influence the cross-talk between bone and glucose homeostasis [37]. Altogether, these studies suggest that EPDR1 potentially acts as a circulating signal to communicate between endocrinologically active tissues such as pancreatic islets, adipose tissue and bone to regulate their cell metabolism and maintain whole-body energy and glucose homeostasis.

In this study, we demonstrated that *EPDR1* is expressed in human pancreatic islets and β-cell models and positively regulates glucose-induced mitochondrial metabolism and GSIS. A previous study using RNAseq analysis to compare gene expression in highly purified cells from fetal vs. adult human pancreatic islets showed that *EPDR1* mRNA levels decrease in adult α-cells but increase in adult β-cells [20]. Moreover, single cell RNAseq analysis of human islets shows a variable degree of *EPDR1* mRNA expression in β-cells but almost absent mRNA expression in other islet cell types [38]. Moreover, a recent study using single-cell transcriptomic analysis of mouse β and α cells sorted from fetal to adult stages found that *Epdr1* was not among the genes

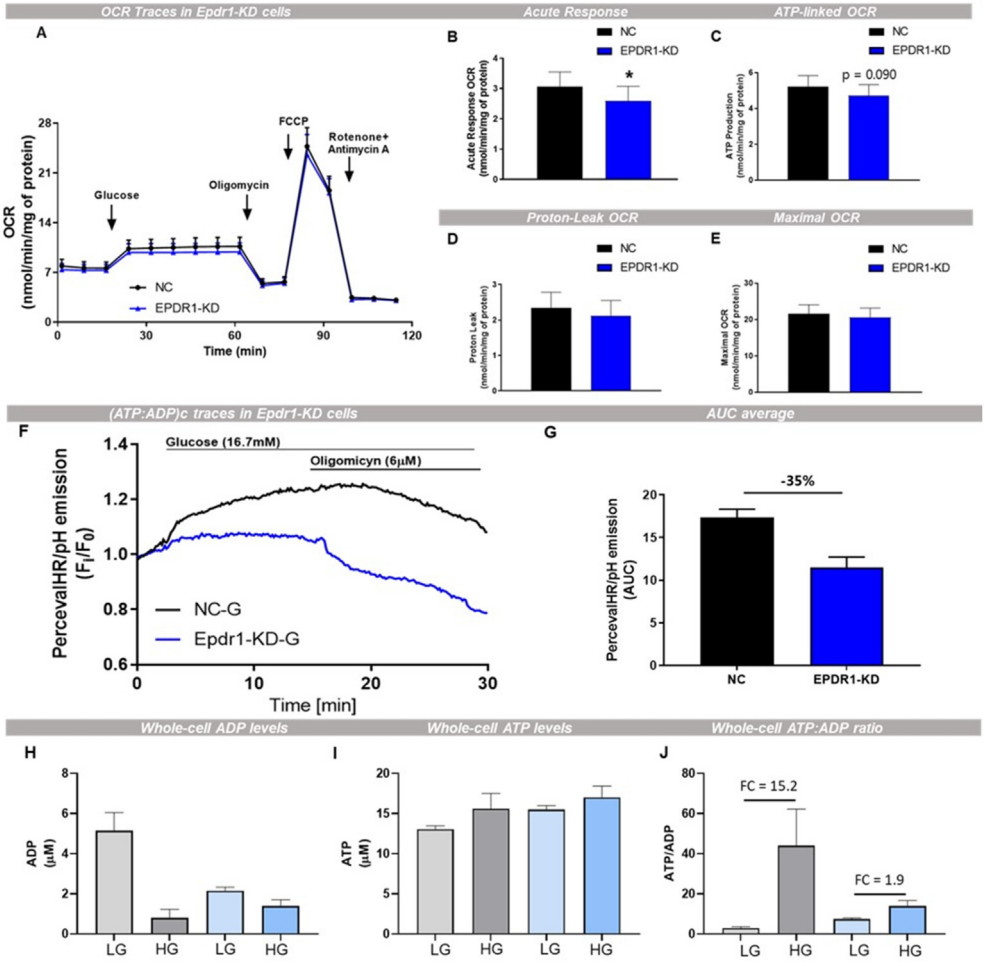

Figure 6: EPDR1 is required for glucose-stimulated increases of ATP/ADP-ratio. (A–E) Mitochondrial Oxygen Consumption Rate (OCR) was measured by Seahorse (XFe24) in INS1 832/13 transfected with scramble or *Epdr1* siRNA (10 nM). (A) Average OCR traces in basal glucose (2.8 mM), glucose (16.7 mM), Oligomycin (4 μM), FCCP (4 μM) and Antimycin A + Rotenone (1 μM) conditions (traces represent average OCR). (B–E) Mitochondrial respiratory parameters; (B) Acute Response OCR, (C) ATP-linked OCR, (D) Proton-Leak OCR and (E) Maximal OCR. Data are mean ± SEM of n = 6 independent experiments. (F–G) Single-cell cytosolic ATP/ADP-ratio (PercevalHR) in response to glucose in *Epdr1*-KD vs NC INS1 832/13 cells. (F) Average traces and (G) Average AUC of traces Data are mean ± SEM of n = 2 independent experiments. (H–J) Whole-cell adenine nucleotides measured by LC-MS in *Epdr1*-KD vs NC INS1 832/13 cells during GSIS (60 min). (H) Whole-cell ADP concentration, (I) Whole-cell ATP concentration and (J) Whole-cell ATP/ADP-ratio. Data are mean ± SEM of n = 4 independent experiments, *p < 0.05 with one-way ANOVA followed by Kruskal Wallis post hoc test.

differentially expressed between β- and α-lineages during the maturation process of mouse pancreatic islet cells [39]. However, they found that *Epdr1* was among the genes variably expressed in adult (P60) β-cells. Pancreatic islets from P60 mice represent the more mature and the less proliferative stage of β-cells; thus, a significant variation of *Epdr1* expression in β-cells may support a role of EPDR1 in β-cell function. These data support the idea that EPDR1 may be selectively expreessed in mature β-cell to positively regulate their function.

In this study we show that *EPDR1* expression was upregulated in pancreatic islets from T2D and obese donors and that its expression was positively correlated with BMI of donors. A linear positive correlation between BMI of ND subjects with both the basal (fasting) and stimulated insulin secretion during oral glucose tolerance test (OGTT) has previously been established [40,41]. This relationship has been further demonstrated by *ex vivo* experiments, assessing dynamics of insulin secretion from pancreatic islets isolated from ND donors, confirming a positive correlation between donor BMI [19–33] and islet insulin content and GSIS [42]. Thus, our observation of an upregulation of *EPDR1* expression in human islets from obese people leads us to propose that *EPDR1* upregulation in human islets from obese people is part of an adaptive program attempting to re-establish glucose homeostasis by increasing β-cell glucose-responsiveness to cope with an increased metabolic demand imposed by insulin resistance. In support of this hypothesis, we also found a strong positive correlation between *EPDR1* mRNA levels and insulin secretion whereas a negative correlation with Hb1Ac was evident. Accordingly, treatment of human pancreatic islets and β-cell models with human EPDR1 protein resulted in increased GSIS whereas silencing of *EPDR1* expression in human islets and INS1 (832/13) cells decreased GSIS.

Interestingly, *EPDR1* is also upregulated in BAT of obese subjects [19] and it has been shown that obese vs lean healthy subjects have elevated fat accumulation in BAT-depots [43] and pancreases [44]. Thus, a potential common signal driving the rise of *EPDR1* expression in pancreatic islet and hBAT could be increased ectopic cellular fat accumulation in subjects with elevated BMI. Notably, *Epdr1* has been

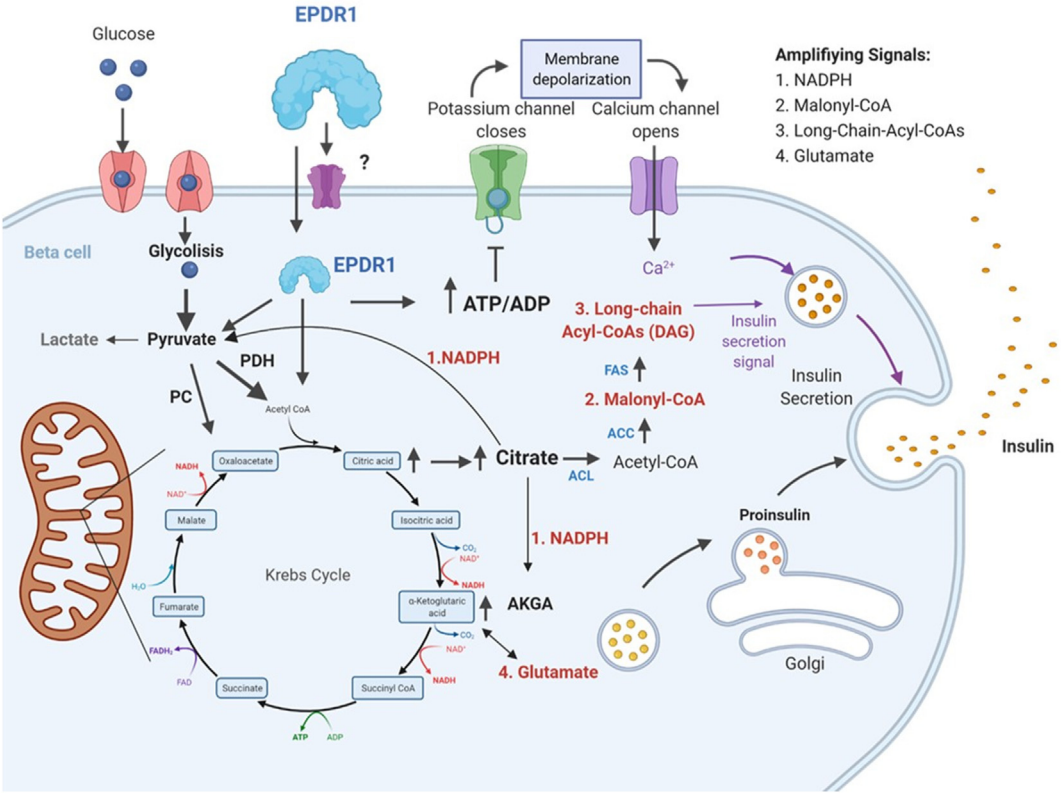

Figure 7: Model of EPDR1 regulation of β-cell metabolism and function. EPDR1 can regulate β-cell metabolism by binding and signaling through a not yet identified plasma membrane receptor or be taken up to act intracellularly. EPDR1 positively regulates GSIS of β-cells by increasing the coupling of glucose metabolism to mitochondrial TCA cycle. EPDR1 is required to channel the glycolysis-derived pyruvate to the TCA cycle, avoiding production of lactate; this results in increased levels of cytosolic ATP/ADP-ratio, which blocks the K_{ATP} channels, raises calcium influx and triggers the insulin granule exocytosis. Additionally, EPDR1 may positively regulate GSIS by increasing the mitochondrial production of TCA cycle-derived citrate, which would be exported to the cytosol and act as precursors of metabolic coupling factors such as NADPH, Malonyl-CoA, long chain acyl-CoAs or Glutamate; these are all metabolites that positively regulate insulin granule exocytosis. PDH: Pyruvate dehydrogenase, PC: Pyruvate Carboxylase, AKGA: Alpha-ketoglutaric acid.

recently identified as a target gene of a non-canonical insulin signaling in endothelial cells [45]. Thus, another potential explanation for the observed positive correlation between *EPDR1* expression and donors BMI maybe the obesity-associated hyperinsulinemia.

We observed that long-term treatment of both human and rodent β-cell lines with the human EPDR1 protein resulted in an inverted "U-Shaped" dose-effect on GSIS, namely, EPDR1 positively affect GSIS reaching a peak at intermediate tested doses (2.5—5.0 μg/ml) whereas losing its effect at the highest tested doses (10 μg/mL). Even though a plasma membrane receptor for EPDR1 has not been identified so far, this inverted "U-Shaped" dose-effect of EPDR1 on GSIS may suggest that EPDR1 signaling through a plasma membrane receptor in β-cells is desensitized by reducing its expression or translocation to the plasma membrane ligand concentrations are saturated. An alternative explanation could be that long-term activation of EPDR1-dependent signaling in β-cells may result in increased production of oxidative stress at the mitochondrial ETC level; this may become detrimental to β-cell function as we have observed previously for a serotonin receptor, which acutely increases GSIS but conversely, after long-term stimulation decreases GSIS [46].

We identified eQTLs for *EPDR1* in suggestive association with two *ex vivo* parameters of β-cell function: GSIS stimulatory index and GLP1-promoted GSIS. This is a relevant finding since linking genetic variation with *EPDR1* expression in human islets and β-cell function may be useful to translate these *in vitro* results to human epidemiological studies. For example, it may reveal whether *EPDR1* expression in human β-cells, based on subject's eQTLs genotype, is associated with *in vivo* β-cell function and glucose homeostatic traits (derived from OGTT) and T2D incidence/prognosis.

By use of a metabolomic approach, we found evidence for EPDR1 contributing to a tightening of the coupling of glycolysis to mitochondrial TCA-cycle metabolism, a mechanism underlying its positive regulation of GSIS (Figure 7). We have demonstrated that *Epdr1* silencing in β-cells resulted in a Warburg effect (i.e. diverting glycolysis-derived pyruvate from mitochondria to lactate production) and reduced activity of the malate-aspartate shuttle and reduction in the TCA cycle metabolite levels. Re-oxidation of the cytosolic NADH is required to maintain glycolytic and TCA cycle flux [47,48]. In most cells NADH is recovered by the lactate dehydrogenase A (*LDHA*)-mediated reduction of pyruvate to lactate. However, *LDHA* is a disallowed/forbidden gene in β-cells [49,50]. In β-cells, the cytosolic NADH re-oxidation relies on two metabolic redox systems: the malate-aspartate shuttle and the glycerol-phosphate (GP) shuttle [48]. The findings in our metabolomics analysis of *Epdr1*-KD cells are compatible with a model where defects in the transfer of reducing potential from glycolysis to TCA cycle by the malate-aspartate shuttle forces the activation of LDHA, resulting in a decreased supply of substrates to TCA-cycle. Increased metabolic flux of glucose-derived pyruvate into the TCA cycle increases GSIS [51].

Conversely, impaired glucose-responsiveness and GSIS are often accompanied with disturbed coupling of glycolytic and TCA cycle mitochondrial metabolism and increased lactate production [52]. Consistently, we have shown increased glucose-stimulated lactate cell content and secretion from *Epdr1*-KD cells, supporting an activation of the anaerobic glycolysis pathway.

Ample evidence support that disturbance of mitochondrial metabolism is a cause of β-cell dysfunction in different models of diabetes [3]. In this study we showed that *Epdr1* silencing reduced glucose-stimulated mitochondrial respiration and decreased the cytosolic and the whole-cell ATP/ADP-ratio. In addition, we observed that *Epdr1* silencing increased the content of mitochondrial ETC proteins, which may reflect compensatory biogenesis of mitochondria replacing defective mitochondria [53]. These data indicated defective glucose-stimulated mitochondrial activity upon *Epdr1* silencing in β-cells (Figure 7).

Interestingly, a recent study has demonstrated that pyruvate kinase, rather than mitochondrial oxidative phosphorylation, is the main driver of the cytosolic ATP/ADP-ratio to close β-cell K_{ATP} channels and initiate insulin secretion [54]. Thus, an alternative explanation to such strong reduced cytosolic ATP/ADP-ratio we observed in the *Epdr1* deficient cells, could be a reduced anaplerotic capacity of mitochondria to produce phosphoenolpyruvate required for the pyruvate kinase-mediated synthesis of ATP. Together, our data indicated that EPDR1 is positively regulating GSIS by a metabolic mechanism tightening the coupling of glycolysis to mitochondrial TCA cycle; this contributes to an adequate glucose-stimulated rise in the cytosolic ATP/ADP-ratio (Figure 7).

5. CONCLUSION

EPDR1 expression in β-cells may increase under metabolic overload (obesity), channelling glycolysis-derived pyruvate to the mitochondrial TCA cycle and, consequently enhance stimulus-secretion coupling and increasing GSIS. Upregulation of EPDR1 expression in pancreatic islets from obese people may reduce their risk to progress from glucose intolerance to T2D.

FUNDING

This work was supported by Novo Nordisk Foundation (NNF18CC0034900), Knut and Alice Wallenberg Foundation (KAW2018.0094), Swedish Research Council (2021-01777 and 2019-01406), The Royal Physiographic Society of Lund (41521-2020 and 42009-2021) and Bo & Kerstin Hjelt Diabetes Foundation. The Novo Nordisk Leif Groop Young-Scientist Scholarship. The laboratory is part of the LUDC-IRC and was supported by the Swedish Foundation for Strategic Research Dnr IRC15-0067.

DUALITY OF INTEREST

No potential conflicts of interest relevant to this article were reported.

AUTHORSHIP CONTRIBUTIONS

L.R.C. conceptualized and designed this study. L.R.C., L.A., O.H., E.C., S.H., S.G. performed experiments and analyzed data. R.*P. and* Q.G. performed statistical data análisis and assisted with experimental design. P.S., C.S., M.F., H.M. and T.M., L.E. contributed to the interpretation and discussion of data. L.R.C., TM and H.M. wrote the manuscript. All authors revised the manuscript and approved the final version to be published. L.R.C. is the guarantor of this work and, as such, had full access to all the data in the study and takes responsibility for the integrity of the data and the accuracy of the data analysis.

PRIOR PRESENTATION

Preliminary results of this study were presented at the 57th Annual Meeting of the EASD (poster #378), Sept 27-Oct 1-2021.

DATA AVAILABILITY

Data will be made available on request.

ACKNOWLEDGEMENTS

We thank the Nordic Network for Clinical Islet Transplantation (JDRF award 31 2008 416) , the tissue isolation teams and Human Tissue Laboratory within EXODIAB/Lund University Diabetes Center. We also thank Emeritus Professor Claes Wollheim (Lund University) for fruitful scientific discussions and Anna-Maria Veljanovska Ramsay and Laila Jacobsson (Lund University) for technical assistance.

CONFLICT OF INTEREST

None declared.

APPENDIX A. SUPPLEMENTARY DATA

Supplementary data to this article can be found online at https://doi.org/10.1016/j.molmet.2022.101629.

REFERENCES

[1] Maechler, P., Wollheim, C.B., 2001. Mitochondrial function in normal and diabetic beta-cells. Nature 414(6865):807–812.

[2] Malmgren, S., Nicholls, D.G., Taneera, J., Bacos, K., Koeck, T., Tamaddon, A., et al., 2009. Tight coupling between glucose and mitochondrial metabolism in clonal beta-cells is required for robust insulin secretion. Journal of Biological Chemistry 284(47):32395–32404.

[3] Haythorne, E., Rohm, M., van de Bunt, M., Brereton, M.F., Tarasov, A.I., Blacker, T.S., et al., 2019. Diabetes causes marked inhibition of mitochondrial metabolism in pancreatic beta-cells. Nature Communications 10(1):2474.

[4] Apostolopoulos, J., Sparrow, R.L., McLeod, J.L., Collier, F.M., Darcy, P.K., Slater, H.R., et al., 2001. Identification and characterization of a novel family of mammalian ependymin-related proteins (MERPs) in hematopoietic, non-hematopoietic, and malignant tissues. DNA and Cell Biology 20(10):625–635.

[5] Nimmrich, I., Erdmann, S., Melchers, U., Chtarbova, S., Finke, U., Hentsch, S., et al., 2001. The novel ependymin related gene UCC1 is highly expressed in colorectal tumor cells. Cancer Letters 165(1):71–79.

[6] Riffo-Campos, A.L., Castillo, J., Vallet-Sanchez, A., Ayala, G., Cervantes, A., Lopez-Rodas, G., et al., 2016. In silico RNA-seq and experimental analyses reveal the differential expression and splicing of EPDR1 and ZNF518B genes in relation to KRAS mutations in colorectal cancer cells. Oncology Reports 36(6):3627–3634.

[7] Gimeno-Valiente, F., Riffo-Campos, A.L., Ayala, G., Tarazona, N., Gambardella, V., Rodriguez, F.M., et al., 2020. EPDR1 up-regulation in human colorectal cancer is related to staging and favours cell proliferation and invasiveness. Scientific Reports 10(1):3723.

[8] Chen, R., Zhang, Y., 2020. EPDR1 correlates with immune cell infiltration in hepatocellular carcinoma and can be used as a prognostic biomarker. Journal of Cellular and Molecular Medicine 24(20):12107–12118.

[9] Park, S., Daily, J.W., Song, M.Y., Kwon, H.K., 2020. Gene-gene and gene-lifestyle interactions of AKAP11, KCNMA1, PUM1, SPTBN1, and EPDR1 on osteoporosis risk in middle-aged adults. Nutrition 79–80:110859.

[10] Staats, K.A., Wu, T., Gan, B.S., O'Gorman, D.B., Ophoff, R.A., 2016. Dupuytren's disease susceptibility gene, EPDR1, is involved in myofibroblast contractility. Journal of Dermatological Science 83(2):131–137.

[11] Ng, M., Thakkar, D., Southam, L., Werker, P., Ophoff, R., Becker, K., et al., 2017. A genome-wide association study of dupuytren disease reveals 17 additional variants implicated in fibrosis. The American Journal of Human Genetics 101(3):417–427.

[12] Khor, C.C., Do, T., Jia, H., Nakano, M., George, R., Abu-Amero, K., et al., 2016. Genome-wide association study identifies five new susceptibility loci for primary angle closure glaucoma. Nature Genetics 48(5):556–562.

[13] Wiggs, J.L., Pasquale, L.R., 2017. Genetics of glaucoma. Human Molecular Genetics 26(R1):R21–R27.

[14] Wei, Y., Xiong, Z.J., Li, J., Zou, C., Cairo, C.W., Klassen, J.S., et al., 2019. Crystal structures of human lysosomal EPDR1 reveal homology with the superfamily of bacterial lipoprotein transporters. Communication Biology 2: 52.

[15] Kollmann, K., Mutenda, K.E., Balleininger, M., Eckermann, E., von Figura, K., Schmidt, B., et al., 2005. Identification of novel lysosomal matrix proteins by proteome analysis. Proteomics 5(15):3966–3978.

[16] Sleat, D.E., Wang, Y., Sohar, I., Lackland, H., Li, Y., Li, H., et al., 2006. Identification and validation of mannose 6-phosphate glycoproteins in human plasma reveal a wide range of lysosomal and non-lysosomal proteins. Molecular & Cellular Proteomics 5(10):1942–1956.

[17] Sleat, D.E., Zheng, H., Lobel, P., 2007. The human urine mannose 6-phosphate glycoproteome. Biochimica et Biophysica Acta 1774(3):368–372.

[18] Della Valle, M.C., Sleat, D.E., Sohar, I., Wen, T., Pintar, J.E., Jadot, M., et al., 2006. Demonstration of lysosomal localization for the mammalian ependymin-related protein using classical approaches combined with a novel density shift method. Journal of Biological Chemistry 281(46):35436–35445.

[19] Deshmukh, A.S., Peijs, L., Beaudry, J.L., Jespersen, N.Z., Nielsen, C.H., Ma, T., et al., 2019. Proteomics-based comparative mapping of the secretomes of human Brown and white adipocytes reveals EPDR1 as a novel batokine. Cell Metabolism 30(5):963–975 e7.

[20] Blodgett, D.M., Nowosielska, A., Afik, S., Pechhold, S., Cura, A.J., Kennedy, N.J., et al., 2015. Novel observations from next-generation RNA sequencing of highly purified human adult and fetal islet cell subsets. Diabetes 64(9):3172–3181.

[21] Asplund, O., Storm, P., Chandra, V., Hatem, G., Ottosson-Laakso, E., Mansour-Aly, D., et al., 2022. Islet Gene View-a tool to facilitate islet research. Life Sci Alliance 5(12).

[22] Hohmeier, H.E., Mulder, H., Chen, G., Henkel-Rieger, R., Prentki, M., Newgard, C.B., 2000. Isolation of INS-1-derived cell lines with robust ATP-sensitive K+ channel-dependent and -independent glucose-stimulated insulin secretion. Diabetes 49(3):424–430.

[23] Ravassard, P., Hazhouz, Y., Pechberty, S., Bricout-Neveu, E., Armanet, M., Czernichow, P., et al., 2011. A genetically engineered human pancreatic beta cell line exhibiting glucose-inducible insulin secretion. Journal of Clinical Investigation 121(9):3589–3597.

[24] Taneera, J., Fadista, J., Ahlqvist, E., Atac, D., Ottosson-Laakso, E., Wollheim, C.B., et al., 2015. Identification of novel genes for glucose metabolism based upon expression pattern in human islets and effect on insulin secretion and glycemia. Human Molecular Genetics 24(7):1945–1955.

[25] Sato, S., Dyar, K.A., Treebak, J.T., Jepsen, S.L., Ehrlich, A.M., Ashcroft, S.P., et al., 2022. Atlas of exercise metabolism reveals time-dependent signatures of metabolic homeostasis. Cell Metabolism 34(2):329–345 e8.

[26] Tantama, M., Martinez-Francois, J.R., Mongeon, R., Yellen, G., 2013. Imaging energy status in live cells with a fluorescent biosensor of the intracellular ATP-to-ADP ratio. Nature Communications 4:2550.

[27] Johnson, W.E., Li, C., Rabinovic, A., 2007. Adjusting batch effects in microarray expression data using empirical Bayes methods. Biostatistics 8(1): 118–127.

[28] Vinuela, A., Varshney, A., van de Bunt, M., Prasad, R.B., Asplund, O., Bennett, A., et al., 2020. Genetic variant effects on gene expression in human pancreatic islets and their implications for T2D. Nature Communications 11(1):4912.

[29] Drucker, D.J., 2006. The biology of incretin hormones. Cell Metabolism 3(3): 153–165.

[30] Lawlor, N., Marquez, E.J., Orchard, P., Narisu, N., Shamim, M.S., Thibodeau, A., et al., 2019. Multiomic profiling identifies cis-regulatory networks underlying human pancreatic beta cell identity and function. Cell Rep 26(3):788–801 e6.

[31] Hall, E., Dekker Nitert, M., Volkov, P., Malmgren, S., Mulder, H., Bacos, K., et al., 2018. The effects of high glucose exposure on global gene expression and DNA methylation in human pancreatic islets. Molecular and Cellular Endocrinology 472:57–67.

[32] Gheni, G., Ogura, M., Iwasaki, M., Yokoi, N., Minami, K., Nakayama, Y., et al., 2014. Glutamate acts as a key signal linking glucose metabolism to incretin/cAMP action to amplify insulin secretion. Cell Rep 9(2):661–673.

[33] Chu, C.H., Chang, S.C., Wang, H.H., Yang, S.H., Lai, K.C., Lee, T.C., 2018. Prognostic values of EPDR1 hypermethylation and its inhibitory function on tumor invasion in colorectal cancer. Cancers 10(10).

[34] Yang, Y., Zhang, H., Liu, Z., Zhao, F., Liang, G., 2021. EPDR1 is related to stages and metastasize in bladder cancer and can be used as a prognostic biomarker. BMC Urology 21(1):71.

[35] Wei, H., Liu, L., Chen, Q., 2015. Selective removal of mitochondria via mitophagy: distinct pathways for different mitochondrial stresses. Biochimica et Biophysica Acta 1853(10 Pt B):2784–2790.

[36] Pippin, J.A., Chesi, A., Wagley, Y., Su, C., Pahl, M.C., Hodge, K.M., et al., 2021. CRISPR-Cas9-Mediated genome editing confirms EPDR1 as an effector gene at the BMD GWAS-implicated 'STARD3NL' locus. JBMR Plus 5(9): e10531.

[37] Cipriani, C., Colangelo, L., Santori, R., Renella, M., Mastrantonio, M., Minisola, S., et al., 2020. The interplay between bone and glucose metabolism. Frontiers in Endocrinology 11:122.

[38] Lawlor, N., George, J., Bolisetty, M., Kursawe, R., Sun, L., Sivakamasundari, V., et al., 2017. Single-cell transcriptomes identify human islet cell signatures and reveal cell-type-specific expression changes in type 2 diabetes. Genome Research 27(2):208–222.

[39] Qiu, W.L., Zhang, Y.W., Feng, Y., Li, L.C., Yang, L., Xu, C.R., 2017. Deciphering pancreatic islet beta cell and alpha cell maturation pathways and characteristic features at the single-cell level. Cell Metabolism 25(5):1194–11205 e4.

[40] Ferrannini, E., Mari, A., 2004. Beta cell function and its relation to insulin action in humans: a critical appraisal. Diabetologia 47(5):943–956.

[41] Polonsky, K.S., Given, B.D., Hirsch, L., Shapiro, E.T., Tillil, H., Beebe, C., et al., 1988. Quantitative study of insulin secretion and clearance in normal and obese subjects. Journal of Clinical Investigation 81(2):435–441.

[42] Henquin, J.C., 2018. Influence of organ donor attributes and preparation characteristics on the dynamics of insulin secretion in isolated human islets. Physiological Reports 6(5).

[43] Leitner, B.P., Huang, S., Brychta, R.J., Duckworth, C.J., Baskin, A.S., McGehee, S., et al., 2017. Mapping of human brown adipose tissue in lean and obese young men. Proceedings of the National Academy of Sciences of the U S A 114(32):8649–8654.

[44] Saisho, Y., Butler, A.E., Meier, J.J., Monchamp, T., Allen-Auerbach, M., Rizza, R.A., et al., 2007. Pancreas volumes in humans from birth to age one hundred taking into account sex, obesity, and presence of type-2 diabetes. Clinical Anatomy 20(8):933–942.

[45] Ahmed, T., Flores, P.C., Pan, C.C., Ortiz, H.R., Lee, Y.S., Langlais, P.R., et al., 2022. EPDR1 is a noncanonical effector of insulin-mediated angiogenesis regulated by an endothelial-specific TGF-beta receptor complex. Journal of Biological Chemistry 298(9):102297.

[46] Cataldo, L.R., Mizgier, M.L., Bravo Sagua, R., Jana, F., Cardenas, C., Llanos, P., et al., 2017. Prolonged activation of the Htr2b serotonin receptor impairs glucose stimulated insulin secretion and mitochondrial function in MIN6 cells. PLoS One 12(1):e0170213.

[47] Jitrapakdee, S., Wutthisathapornchai, A., Wallace, J.C., MacDonald, M.J., 2010. Regulation of insulin secretion: role of mitochondrial signalling. Diabetologia 53(6):1019–1032.

[48] Eto, K., Tsubamoto, Y., Terauchi, Y., Sugiyama, T., Kishimoto, T., Takahashi, N., et al., 1999. Role of NADH shuttle system in glucose-induced activation of mitochondrial metabolism and insulin secretion. Science 283(5404):981–985.

[49] Quintens, R., Hendrickx, N., Lemaire, K., Schuit, F., 2008. Why expression of some genes is disallowed in beta-cells. Biochemical Society Transactions 36(Pt 3):300–305.

[50] Pullen, T.J., Khan, A.M., Barton, G., Butcher, S.A., Sun, G., Rutter, G.A., 2010. Identification of genes selectively disallowed in the pancreatic islet. Islets 2(2):89–95.

[51] Krus, U., Kotova, O., Spegel, P., Hallgard, E., Sharoyko, V.V., Vedin, A., et al., 2010. Pyruvate dehydrogenase kinase 1 controls mitochondrial metabolism and insulin secretion in INS-1 832/13 clonal beta-cells. Biochemical Journal 429(1):205–213.

[52] Spegel, P., Malmgren, S., Sharoyko, V.V., Newsholme, P., Koeck, T., Mulder, H., 2011. Metabolomic analyses reveal profound differences in glycolytic and tricarboxylic acid cycle metabolism in glucose-responsive and -unresponsive clonal beta-cell lines. Biochemical Journal 435(1):277–284.

[53] Johansson, P.A., Brattas, P.L., Douse, C.H., Hsieh, P., Adami, A., Pontis, J., et al., 2022. A cis-acting structural variation at the ZNF558 locus controls a gene regulatory network in human brain development. Cell Stem Cell 29(1):52–69 e8.

[54] Lewandowski, S.L., Cardone, R.L., Foster, H.R., Ho, T., Potapenko, E., Poudel, C., et al., 2020. Pyruvate kinase controls signal strength in the insulin secretory pathway. Cell Metabolism 32(5):736–750 e5.

